

Algebraic Sub-structuring for Electromagnetic Applications

Chao Yang¹, Weiguo Gao¹, Zhaojun Bai², Xiaoye S. Li¹, Lie-Quan Lee³,
Parry Husbands¹, and Esmond G. Ng¹

¹ Computational Research Division
Lawrence Berkeley National Lab
Berkeley CA 94720, USA

{CYang, WGGao, XSLi, PJRHusbands, EGNg}@lbl.gov

² Department of Computer Science
The University of California at Davis
Davis, CA 95616, USA
bai@cs.ucdavis.edu

³ Stanford Linear Accelerator Center
Menlo Park, CA 94025, USA
liequan@slac.stanford.edu

Abstract. Algebraic sub-structuring refers to the process of applying matrix re-ordering and partitioning algorithms to divide a large sparse matrix into smaller submatrices from which a subset of spectral components are extracted and combined to form approximate solutions to the original problem. In this paper, we show that algebraic sub-structuring can be effectively used to solve generalized eigenvalue problems arising from the finite element analysis of an accelerator structure.

1 Introduction

Sub-structuring is a commonly used technique for studying the static and dynamic properties of large engineering structures [3,6,11]. The basic idea of sub-structuring is analogous to the concept of domain-decomposition widely used in the numerical solution of partial differential equations [13]. By dividing a large structure model or computational domain into a few smaller components (sub-structures), one can often obtain an approximate solution to the original problem from a linear combination of solutions to similar problems defined on the sub-structures. Because solving problems on each sub-structure requires far less computational power than what would be required to solve the entire problem as a whole, sub-structuring can lead to a significant reduction in the computational time required to carry out a large-scale simulation and analysis.

The automated multi-level sub-structuring (AMLS) method introduced in [1,7] is an extension of a simple sub-structuring method called *component mode synthesis* (CMS) [3,6] originally developed in the 1960s to solve large-scale eigenvalue problems. The method has been used successfully in the vibration and acoustic analysis of large-scale finite element models of automobile bodies [7,9]. The timing results reported in [7,9] indicate that AMLS is significantly faster than conventional Lanczos-based approaches

[10,5]. However, it is important to note that the accuracy achieved by a sub-structuring method such as AMLS is typically lower than that achieved by the standard Lanczos algorithm. The method is most valuable when a large number of eigenpairs with relatively low accuracy are of interest.

In [15], we examined sub-structuring methods for solving large-scale eigenvalue problems from a purely algebraic point of view. We used the term *algebraic sub-structuring* to refer to the process of applying matrix reordering and partitioning algorithms (such as the *nested dissection* algorithm [4]) to divide a large sparse matrix into smaller submatrices from which a subset of spectral components are extracted and combined to form an approximate solution to the original eigenvalue problem. Through an algebraic manipulation, we identified the critical conditions under which algebraic sub-structuring works well. In particular, we observed an interesting connection between the accuracy of an approximate eigenpair obtained through sub-structuring and the distribution of components of eigenvectors associated with a canonical matrix pencil congruent to the original problem. We developed an error estimate for the approximation to the smallest eigenpair, which we will summarize in this paper. The estimate leads to a simple heuristic for choosing spectral components from each sub-structure.

Our interest in algebraic sub-structuring is motivated in part by an application arising from the simulation of the electromagnetic field associated with next generation particle accelerator design [8]. We show in this paper that algebraic sub-structuring can be used effectively to compute the cavity resonance frequencies and the electromagnetic field generated by a linear particle accelerator model.

Throughout this paper, capital and lower case Latin letters denote matrices and vectors respectively, while lower case Greek letters denote scalars. An $n \times n$ identity matrix will be denoted by I_n . The j -th column of the identity matrix is denoted by e_j . The transpose of a matrix A is denoted by A^T . We use $\|x\|$ to denote the standard 2-norm of x , and use $\|x\|_M$ to denote the M -norm defined by $\|x\|_M = \sqrt{x^T M x}$. We will use $\angle_M(x, y)$ to denote the M -inner product induced acute angle (M -angle for short) between x and y . This angle can be computed from $\cos \angle_M(x, y) = x^T M y / \|x\|_M \|y\|_M$. A matrix pencil (K, M) is said to be *congruent* to another pencil (A, B) if there exists a nonsingular matrix P , such that $A = P^T K P$ and $B = P^T M P$.

2 Algebraic Sub-structuring

In this section, we briefly describe a single-level algebraic sub-structuring algorithm. This is also known as the *component synthesis method* (CMS) in the engineering literature [6]. Our description does not make use of any information regarding the geometry or the physical structure on which the original problem is defined.

We are concerned with solving the following generalized algebraic eigenvalue problem

$$Kx = \lambda Mx, \quad (2.1)$$

where K is symmetric and M is symmetric positive definite. We assume K and M are both sparse. They may or may not have the same sparsity pattern. Suppose the rows and columns of K and M have been permuted so that these matrices can be partitioned as

$$K = \begin{matrix} & \begin{matrix} n_1 & n_2 & n_3 \end{matrix} \\ \begin{matrix} n_1 \\ n_2 \\ n_3 \end{matrix} & \begin{pmatrix} K_{11} & & K_{13} \\ & K_{22} & K_{23} \\ K_{13}^T & K_{23}^T & K_{33} \end{pmatrix} \end{matrix} \quad \text{and} \quad M = \begin{matrix} & \begin{matrix} n_1 & n_2 & n_3 \end{matrix} \\ \begin{matrix} n_1 \\ n_2 \\ n_3 \end{matrix} & \begin{pmatrix} M_{11} & & M_{13} \\ & M_{22} & M_{23} \\ M_{13}^T & M_{23}^T & M_{33} \end{pmatrix} \end{matrix}, \quad (2.2)$$

where the labels n_1, n_2 and n_3 denote the dimensions of each sub-matrix block. The permutation can be accomplished by applying a matrix ordering and partitioning algorithm such as the nested dissection algorithm [4] to the matrix $K + M$.

The pencils (K_{11}, M_{11}) and (K_{22}, M_{22}) now define two algebraic sub-structures that are connected by the third block rows and columns of K and M which we will refer to as the *interface* block. We assume that n_3 is much smaller than n_1 and n_2 .

A single-level algebraic sub-structuring algorithm proceeds by performing a block factorization

$$K = LDL^T, \quad (2.3)$$

where

$$L = \begin{pmatrix} I_{n_1} & & \\ & I_{n_2} & \\ K_{13}^T K_{11}^{-1} & K_{23}^T K_{22}^{-1} & I_{n_3} \end{pmatrix} \quad \text{and} \quad D = \begin{pmatrix} K_{11} & & \\ & K_{22} & \\ & & \hat{K}_{33} \end{pmatrix}.$$

The last diagonal block of D , often known as the *Schur complement*, is defined by

$$\hat{K}_{33} = K_{33} - K_{13}^T K_{11}^{-1} K_{13} - K_{23}^T K_{22}^{-1} K_{23}.$$

The inverse of the lower triangular factor L defines a congruence transformation that, when applied to the matrix pencil (K, M) , yields a new matrix pencil (\hat{K}, \hat{M}) :

$$\hat{K} = L^{-1}KL^{-T} = D \quad \text{and} \quad \hat{M} = L^{-1}ML^{-T} = \begin{pmatrix} M_{11} & & \hat{M}_{13} \\ & M_{22} & \hat{M}_{23} \\ \hat{M}_{13}^T & \hat{M}_{23}^T & \hat{M}_{33} \end{pmatrix}. \quad (2.4)$$

The pencil (\hat{K}, \hat{M}) is often known as the *Craig-Bampton* form [3] in structural engineering. Note that the eigenvalues of (\hat{K}, \hat{M}) are identical to those of (K, M) , and the corresponding eigenvectors \hat{x} are related to the eigenvectors of the original problem (2.1) through $\hat{x} = L^T x$.

The sub-structuring algorithm constructs a subspace spanned by

$$S = \begin{matrix} & \begin{matrix} k_1 & k_2 & n_3 \end{matrix} \\ \begin{matrix} n_1 \\ n_2 \\ n_3 \end{matrix} & \begin{pmatrix} S_1 & & \\ & S_2 & \\ & & I_{n_3} \end{pmatrix} \end{matrix} \quad (2.5)$$

where S_1 and S_2 consist of k_1 and k_2 selected eigenvectors of (K_{11}, M_{11}) and (K_{22}, M_{22}) respectively. These eigenvectors will be referred to as *sub-structure modes*

in the discussion that follows. Note that k_1 and k_2 are typically much smaller than n_1 and n_2 , respectively.

The approximation to the desired eigenvalues and eigenvectors of the pencil $(\widehat{K}, \widehat{M})$ are obtained by projecting the pencil $(\widehat{K}, \widehat{M})$ onto the subspace spanned by S , i.e., we seek θ and $q \in \mathbb{R}^{k_1+k_2+n_3}$ such that

$$(S^T \widehat{K} S)q = \theta(S^T \widehat{M} S)q. \quad (2.6)$$

It follows from the standard Rayleigh-Ritz theory [12, page 213] that θ serves as an approximation to an eigenvalue of (K, M) , and the vector formed by $z = L^{-T} S q$ is the approximation to the corresponding eigenvector.

One key aspect of the algebraic sub-structuring algorithm is that k_i can be chosen to be much smaller than n_i . Thus, S_i can be computed by a shift-invert Lanczos procedure. The cost of this computation is generally small compared to the rest of the computation, especially when this algorithm is extended to a multi-level scheme. Similarly, because n_3 is typically much smaller than n_1 and n_2 , the dimension of the projected problem (2.6) is significantly smaller than that of the original problem. Thus, the cost of solving (2.6) is also relatively small.

Decisions must be made on how to select eigenvectors from each sub-structure. The selection should be made in such a way that the subspace spanned by the columns of S retains a sufficient amount of spectral information from (K, M) . The process of choosing appropriate eigenvectors from each sub-structure is referred to as *mode selection* [15].

The algebraic sub-structuring algorithm presented here can be extended in two ways. First, the matrix reordering and partitioning scheme used to create the block structure of (2.2) can be applied recursively to (K_{11}, M_{11}) and (K_{22}, M_{22}) respectively to produce a multi-level division of (K, M) into smaller sub-matrices. The reduced computational cost associated with finding selected eigenpairs from these even smaller sub-matrices further improves the efficiency of the algorithm. Second, one may replace I_{n_3} in (2.5) with a subset of eigenvectors of the interface pencil $(\widehat{K}_{33}, \widehat{M}_{33})$. This modification will further reduce the computational cost associated with solving the projected eigenvalue problem (2.6). A combination of these two extensions yields the AMLS algorithm presented in [7]. However, we will limit the scope of our presentation to a single level sub-structuring algorithm in this paper.

3 Accuracy and Error Estimation

One of the natural questions one may ask is how much accuracy we can expect from the approximate eigenpairs obtained through algebraic sub-structuring. The answer to this question would certainly depend on how S_1 and S_2 are constructed in (2.5). This issue is carefully examined in [15]. In this section, we will summarize the error estimate results established in [15].

To simplify the discussion, we will work with the matrix pencil $(\widehat{K}, \widehat{M})$, where \widehat{K} and \widehat{M} are defined in (2.4). As we noted earlier, $(\widehat{K}, \widehat{M})$ and (K, M) have the same set of eigenvalues. If \widehat{x} is an eigenvector of $(\widehat{K}, \widehat{M})$, then $x = L^{-T} \widehat{x}$ is an eigenvector of (K, M) , where L is the transformation defined in (2.3).

If $(\mu_j^{(i)}, v_j^{(i)})$ is the j -th eigenpair of the i -th sub-problem, i.e.,

$$K_{ii}v_j^{(i)} = \mu_j^{(i)}M_{ii}v_j^{(i)},$$

where $(v_j^{(i)})^T M_{ii} v_k^{(i)} = \delta_{j,k}$, and $\mu_j^{(i)}$ has been ordered such that

$$\mu_1^{(i)} \leq \mu_2^{(i)} \leq \dots \leq \mu_{n_i}^{(i)}, \tag{3.7}$$

then we can express \hat{x} as

$$\hat{x} = \begin{pmatrix} V_1 & & \\ & V_2 & \\ & & I_{n_3} \end{pmatrix} \begin{pmatrix} y_1 \\ y_2 \\ y_3 \end{pmatrix}, \tag{3.8}$$

where $V_i = (v_1^{(i)} v_2^{(i)} \dots v_{n_i}^{(i)})$, and $y = (y_1^T, y_2^T, y_3^T)^T \neq 0$.

It is easy to verify that y satisfies the following *canonical* generalized eigenvalue problem

$$\begin{pmatrix} \Sigma_1 & & \\ & \Sigma_2 & \\ & & \widehat{K}_{33} \end{pmatrix} \begin{pmatrix} y_1 \\ y_2 \\ y_3 \end{pmatrix} = \lambda \begin{pmatrix} I_{n_1} & & G_{13} \\ & I_{n_2} & G_{23} \\ G_{13}^T & G_{23}^T & \widehat{M}_{33} \end{pmatrix} \begin{pmatrix} y_1 \\ y_2 \\ y_3 \end{pmatrix}, \tag{3.9}$$

where $\Sigma_i = \text{diag}(\mu_1^{(i)}, \mu_2^{(i)}, \dots, \mu_{n_i}^{(i)})$, $G_{i3} = V_i^T \widehat{M}_{i3}$ for $i = 1, 2$. This pencil is clearly congruent to the pencils $(\widehat{K}, \widehat{M})$ and (K, M) . Thus it shares the same set of eigenvalues with that of (K, M) .

If \hat{x} can be well approximated by a linear combination of the columns of S , as suggested by the description of the the algorithm in Section 2, then the vector y_i ($i = 1, 2$) must contain only a few large entries. All other components of y_i are likely to be small and negligible.

In [15], we showed that

$$|y_i| = \text{diag} \left(\rho_\lambda(\mu_1^{(i)}), \rho_\lambda(\mu_2^{(i)}), \dots, \rho_\lambda(\mu_{n_i}^{(i)}) \right) g^{(i)}, \tag{3.10}$$

where $g^{(i)} = |e_j^T G_{i3} y_3|$, and

$$\rho_\lambda(\omega) = |\lambda/(\omega - \lambda)|. \tag{3.11}$$

When elements of $g^{(i)}$ can be bounded (from above and below) by a moderate constant, the magnitude of $|e_j^T y_i|$ is essentially determined by $\rho_\lambda(\mu_j^{(i)})$ which is called a ρ -factor in [15].

It is easy to see that $\rho_\lambda(\mu_j^{(i)})$ is large when $\mu_j^{(i)}$ is close to λ , and it is small when $\mu_j^{(i)}$ is away from λ . For the smallest eigenvalue (λ_1) of (K, M) , it is easy to show that $\rho_{\lambda_1}(\mu_j^{(i)})$ is monotonically decreasing with respect to j . Thus, if λ_1 is the desired eigenvalue, one would naturally choose the matrix S_i in (2.5) to contain only the leading k_i columns of V_i , for some $k_i \ll n_i$.

If we define h_i by

$$e_j^T h_i = \begin{cases} 0 & \text{for } j \leq k_i, \\ e_j^T y_i & \text{for } k_i < j \leq n_i, \end{cases} \tag{3.12}$$

then following theorem, which we proved in [15], provides an *a priori* error estimate for the Rayleigh-Ritz approximation to (λ_1, \hat{x}_1) from the subspace spanned by columns of S defined in (2.5).

Theorem 1. *Let \widehat{K} and \widehat{M} be the matrices defined in (2.4). Let (λ_i, \hat{x}_i) ($i = 1, 2, \dots, n$) be eigenpairs of the pencil $(\widehat{K}, \widehat{M})$, ordered so that $\lambda_1 < \lambda_2 \leq \dots \leq \lambda_n$. Let (θ_1, u_1) be the Rayleigh-Ritz approximation to (λ_1, \hat{x}_1) from the space spanned by the columns of S defined in (2.5). Then*

$$\theta_1 - \lambda_1 \leq (\lambda_n - \lambda_1)(h_1^T h_1 + h_2^T h_2), \tag{3.13}$$

$$\sin \angle_{\widehat{M}}(u_1, \hat{x}_1) \leq \sqrt{\frac{\lambda_n - \lambda_1}{\lambda_2 - \lambda_1}} \sqrt{h_1^T h_1 + h_2^T h_2}, \tag{3.14}$$

where h_i ($i = 1, 2$) is defined by (3.12).

Theorem 1 indicates that the accuracy of (θ_1, u_1) is proportional to the size of $h_1^T h_1 + h_2^T h_2$, a quantity that provides a cumulative measure of the “truncated” components in (3.8).

If $\rho_{\lambda_1}(\mu_j^{(i)}) < \tau < 1$ holds for $k_i < j \leq n_i$, and if $e_j^T g^{(i)} \leq \gamma$ for some moderate sized constant γ , we can show [15] that $h_1^T h_1 + h_2^T h_2$ can be bounded by a quantity that is independent of the number of non-zero elements in h_i . Consequently, we can establish the following bounds:

$$\frac{\theta_1 - \lambda_1}{\lambda_1} \leq (\lambda_n - \lambda_1)(2\alpha\tau), \tag{3.15}$$

$$\sin \angle_{\widehat{M}}(\hat{x}_1, u_1) \leq \sqrt{\lambda_1 \left(\frac{\lambda_n - \lambda_1}{\lambda_2 - \lambda_1} \right)} \sqrt{2\alpha\tau}, \tag{3.16}$$

where $\alpha = \gamma^2 / \delta$.

We should mention that (3.15) and (3.16) merely provide a qualitative estimate of the error in the Ritz pair (θ_1, u_1) in terms of the threshold τ that may be used as a heuristic in practice to determine which spectral components of a sub-structure should be included in the subspace S defined in (2.5). It is clear from these inequalities that a smaller τ , which typically corresponds to a selection of more spectral components from each sub-structure, leads to a more accurate Ritz pair (θ_1, u_1) .

4 Numerical Experiment

We show by an example that algebraic sub-structuring can be used to compute approximate cavity resonance frequencies and the electromagnetic field associated with a small

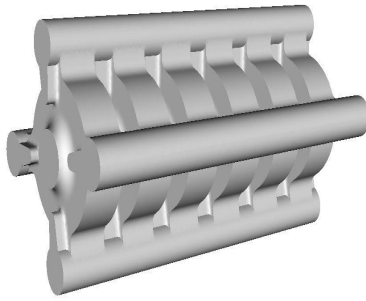


Fig. 1. The finite element model corresponding to a 6-cell damped detuned structure

accelerator structure. The matrix pencil used in this example is obtained from a finite element model of a six-cell Damped Detuned accelerating Structure (DDS) [8]. The three dimensional geometry of the model is shown in Figure 1. The dimension of the pencil (K, M) is $n = 5584$. The stiffness matrix K has 580 zero rows and columns. These zero rows and columns are produced by a particular hierarchical vector finite element discretization scheme [14]. Because K is singular, we cannot perform the block elimination in (2.3) directly. A deflation scheme is developed in [15] to overcome this difficulty. The key idea of the deflation scheme is to replace K_{ii}^{-1} ($i = 1, 2$) with a pseudo-inverse in the congruence transformation calculation. We refer the reader to [15] for the algorithmic details. To facilitate deflation, we perform a two-stage matrix reordering described in [15]. Figure 2 shows the non-zero patterns of the permuted K and M .

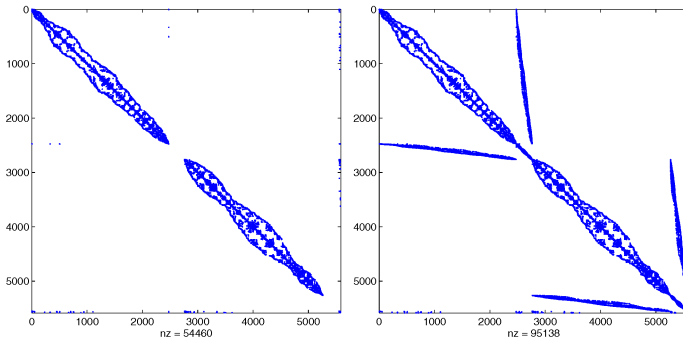


Fig. 2. The non-zero pattern of the permuted stiffness matrix K (left) and the mass matrix M (right) associated with the 6-cell DDS model

We plot the approximate ρ -factors associated with smallest eigenvalue of the deflated problem in Figure 3. The approximation is made by replacing λ_1 (which we do not know in advance) in (3.11) with $\sigma \equiv \min(\mu_1^{(1)}, \mu_1^{(2)})/2$. We showed in [15] that such an approximation does not alter the qualitative behavior of the ρ -factor. Three different

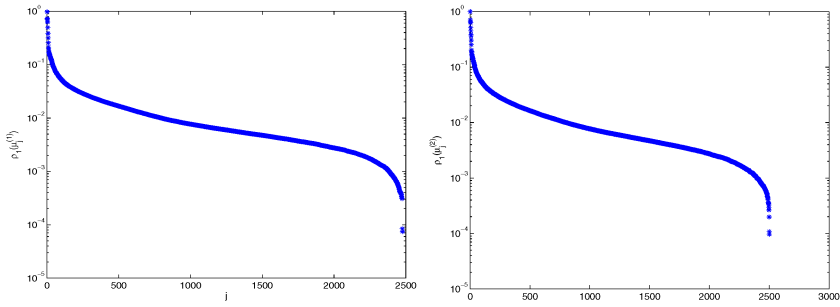


Fig. 3. The approximate ρ -factors associated with each sub-structure of the 6-cell DDS model

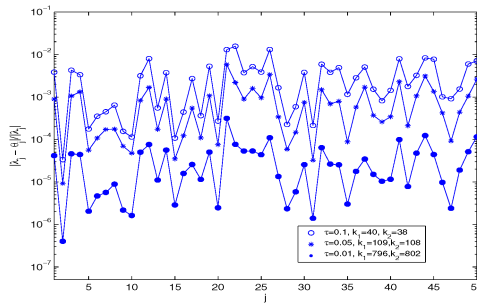


Fig. 4. The relative error of the smallest 50 Ritz values extracted from three subspaces constructed by using different choices of the ρ -factor thresholds (τ values) for the DDS model

choices of τ values were used as the ρ -factor thresholds ($\tau = 0.1, 0.05, 0.01$) for selecting sub-structure modes, i.e., we only select sub-structure modes that satisfy $\rho_\sigma(\mu_j^{(i)}) \geq \tau$.

The relative accuracy of the 50 smallest non-zero Ritz values extracted from the subspaces constructed with these choices of τ values is displayed in Figure 4.

We observe that with $\tau = 0.1$, θ_1 has roughly three digits of accuracy, which is quite sufficient for this particular discretized model. If we decrease τ down to 0.01, most of the smallest 50 non-zero Ritz values have at least 4 to 5 digits of accuracy.

The least upper bound for elements of $g^{(i)}$ used in (3.10) is $\gamma = 0.02$. Thus the ρ -factor gives an over-estimate of elements of $|y_i|$ in this case. In Figure 5, we plot elements of $|y_1|$ and $|y_2|$, where $(y_1^T, y_2^T, y_3^T)^T$ is the eigenvector associated with the smallest non-zero eigenvalue of (3.9). For simplicity, we excluded the elements of $|y_1|$ and $|y_2|$ corresponding to the null space of (K_{11}, M_{11}) and (K_{22}, M_{22}) , which have been deflated from our calculations. We observe that $|e_j^T y_i|$ is much smaller than $\rho_\sigma(\mu_j^{(i)})$, and it decays much faster than the the ρ -factor also.

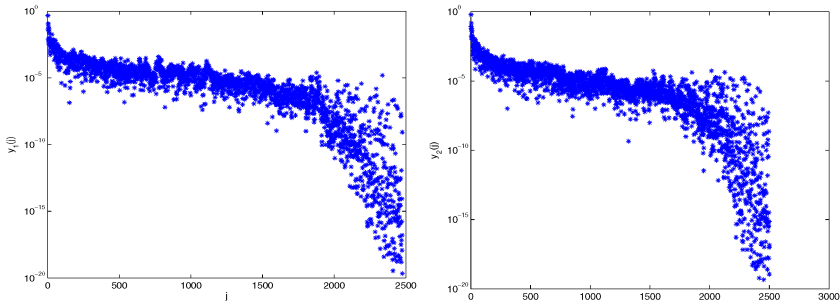


Fig. 5. The magnitude of $|y_1|$ (left) and $|y_2|$ (right) elements, where $(y_1^T, y_2^T, y_3^T)^T$ is the eigenvector corresponding to the smallest eigenvalue of the canonical problem (3.9) associated with the DDS model

5 Concluding Remarks

In this paper, we discussed the possibility of using algebraic sub-structuring to solve large-scale eigenvalue problems arising from electromagnetic simulation. We examined the accuracy of the method based on the analysis developed in [15]. A numerical example is provided to demonstrate the effectiveness of the method.

We should point out that the block elimination and congruence transformation performed in algebraic sub-structuring can be costly in terms of memory usage. However, since no triangular solves on the full matrix, which are typically used in a standard shift-invert Lanczos algorithm, are required, an efficient multi-level out-of-core implementation is possible. We will discuss the implementation issues and comparison with other methods in a future study.

References

1. J. K. Bennighof. Adaptive multi-level substructuring method for acoustic radiation and scattering from complex structures. In A. J. Kalinowski, editor, *Computational methods for Fluid/Structure Interaction*, volume 178, pages 25–38, AMSE, New York, November, 1993.
2. F. Bourquin. Component mode synthesis and eigenvalues of second order operators: Discretization and algorithm. *Mathematical Modeling and Numerical Analysis*, 26:385–423, 1992.
3. R. R. Craig and M. C. C. Bampton. Coupling of substructures for dynamic analysis. *AIAA Journal*, 6:1313–1319, 1968.
4. A. George. Nested dissection of a regular finite element mesh. *SIAM J. Num. Anal.*, 10:345–363, 1973.
5. R. G. Grimes, J. G. Lewis, and H. D. Simon. A shifted block Lanczos algorithm for solving sparse symmetric generalized eigenproblems. *SIAM Journal on Matrix Analysis and Applications*, 15(1):228–272, January 1994.
6. W. C. Hurty. Vibrations of structure systems by component-mode synthesis. *Journal of the Engineering Mechanics Division, ASCE*, 86:51–69, 1960.

7. M. F. Kaplan. *Implementation of Automated Multilevel Substructuring for Frequency Response Analysis of Structures*. PhD thesis, University of Texas at Austin, Austin, TX, December 2001.
8. K. Ko, N. Folwell, L. Ge, A. Guetz, V. Ivanov, L. Lee, Z. Li, I. Malik, W. Mi, C. Ng, and M. Wolf. Electromagnetic systems simulation - from simulation to fabrication. SciDAC report, Stanford Linear Accelerator Center, Menlo Park, CA, 2003.
9. A. Kropp and D. Heiserer. Efficient broadband vibro-accoustic analysis of passenger car bodies using an FE-based component mode synthesis approach. In *Proceedings of the fifth World Congress on Computational Mechanics (WCCM V)*, Vienna University of Technology, 2002.
10. R. B. Lehoucq, D. C. Sorensen, and C. Yang. *ARPACK Users' Guide – Solution of Large-scale eigenvalue problems with implicitly restarted Arnoldi Methods*. SIAM, Philadelphia, PA., 1999.
11. R. H. MacNeal. Vibrations of composite systems. Technical Report OSRTN-55-120, Office of Scientific Research, Air Research of Scientific Research and Development Command, 1954.
12. B. N. Parlett. *The Symmetric Eigenvalue Problem*. Prentice-Hall, 1980.
13. B. Smith, P. Bjørstad, and W. Gropp. *Domain Decomposition*. Cambridge University Press, Cambridge, UK., 1996.
14. Din-Kow Sun, Jin-Fa Lee, and Zoltan Cendes. Construction of nearly orthogonal Nedelec bases for rapid convergence with multilevel preconditioned solvers. *SIAM Journal on Scientific Computing*, 23(4):1053–1076, 2001.
15. C. Yang, W. Gao, Z. Bai, X. Li, L. Lee, P. Husbands, and E. G. Ng. An Algebraic Sub-structuring Algorithm for Large-scale Eigenvalue Calculation. *Technical Report, LBNL-55055*, Submitted to SIAM Journal on Scientific Computing.